FOURIER DOMAIN DISPLAY COLOR FILTER ARRAY DESIGN

Keigo Hirakawa and Patrick J. Wolfe,

Harvard University
Department of Statistics, School of Engineering and Applied Sciences
Oxford Street, Cambridge, MA 02138 USA
{hirakawa, wolfe}@stat.harvard.edu

ABSTRACT

In digital image display devices, data are typically presented via a spatial subsampling procedure implemented as a color filter array, a physical construction whereby each light emitting element controls the intensity level of only a single color. In this paper, we examine the problem of color filter array design with respect to spatial resolution and human vision; in doing so we quantify the fundamental limitations of existing designs by explicitly considering the spectral wavelength representation induced by the choice of array pattern, and propose a framework for designing and analyzing alternative patterns that minimize aliasing. An empirical evaluations on standard color test image confirms our theoretical results, and indicates the potential of these patterns to significantly increase spatial resolution while at the same time improving color image fidelity.

Index Terms— Displays, color measurement, image sampling

1. INTRODUCTION

In digital image display devices, data are typically presented at a subpixel level via a spatial subsampling procedure implemented as a color filter array (CFA), a physical construction whereby each light emitting element controls the intensity level of only a single color. The image formation of display in human vision is often modeled by the contrast sensitivity function (CSF) [1, 2], which has a low-pass effect to filter out the granularity of individual elements, and the use of the CFA patterns is ubiquitous in today's cathode-ray tube, plasma, and liquid crystal display media. The most well known of the color schemes involve the canonical primary colors of light: red, green, and blue [3–5]. In some cases, inclusion of a fourth color such as white is considered [6].

Subpixel rendering and anti-aliasing are some well-known techniques to take advantage of the pixel geometry and arrangement to increase the perceived resolution of the display [4, 5]. The maximal resolution of the display, however, is ultimately limited fundamentally by the choice of the pre-determined CFA pattern. More specifically, the bandwidths of the stimuli that drive the intensity level of the subpixel is typically lower than that of the image features we would like to represent. In this paper, we explicitly quantify the information loss associated with the CFA-based image representation in terms of *spectral* wavelength as well as the *spatial* sampling requirements. We then propose a framework for designing and analyzing alternatives to the existing CFA patterns for color image display devices, which overcomes the shortcomings of the previous patterns.

The authors thank Dr. Damon Chandler for his insightful comments on human vision. Patent Pending.

1.1. A Few Definitions

Let $\boldsymbol{n} \in \mathbb{Z}^2$ be location index and $\boldsymbol{x}(\boldsymbol{n}) = (x_1(\boldsymbol{n}), x_2(\boldsymbol{n}), x_3(\boldsymbol{n}))^T$ be the corresponding red, green, blue (RGB) color triple. Given a two-dimensional signal, terminologies such as *frequency* and *spectral* are to be interpreted in the context of two dimensional Fourier transforms, which is also denoted by $\mathcal{F}(\cdot)$. This is not to be confused with *spectral wavelength*, the wavelengths of the light in the sense of color science. This paper is concerned with the design of *CFA*, which is a spatially varying pattern. Although the image data that drive the light emitting element are sometimes referred to as *CFA image* in the literature, we use *stimuli* to avoid confusion with *CFA*, the coding of color which is not dependent on the image signal content.

2. EXISTING CFA PATTERNS

2.1. Fourier Analysis of Display Stimuli

Let $\boldsymbol{M} \in \mathbb{R}^{3\times 3}$ such that $\boldsymbol{y}(\boldsymbol{n}) = \boldsymbol{M}\boldsymbol{x}(\boldsymbol{n}) \in \mathbb{R}^3$ is the linear transformation decomposing the color defined in RGB color space into luminance component $y_1(\boldsymbol{n})$ and two chrominance components $y_2(\boldsymbol{n}), y_3(\boldsymbol{n})$ (e.g. YUV, YIQ, YCbCr [7]). Because the high frequency contents of x_1, x_2, x_3 are highly redundant, it is often accepted that y_2 and y_3 are bandlimited [8–10]. See Figure 1(a-c). This claim is strongly supported by the fact that the Pearson product-moment correlation coefficient of a color image measured between the color channels is typically larger than 0.9 [11]. It is then not surprising that CSF has far wider passband on y_1 when compared to that of y_2 and y_3 [1, 2].

To motivate our analysis, we first examine vertical and diagonal stripe sampling [6, 12]. Let $\boldsymbol{c}(\boldsymbol{n}) = (c_1(\boldsymbol{n}), c_2(\boldsymbol{n}), c_3(\boldsymbol{n}))^T \in \{\boldsymbol{e}_1, \boldsymbol{e}_2, \boldsymbol{e}_3\}$ be the red, green, and blue indicator for CFA color at pixel location $\boldsymbol{n}$, respectively, where $\boldsymbol{e}_i \in \mathbb{R}^3$ denotes the standard basis. The stimuli $\boldsymbol{u}(\boldsymbol{n}) \in \mathbb{R}$ and displayed image $\boldsymbol{v}(\boldsymbol{n}) \in \mathbb{R}^3$ are:

$$\boldsymbol{u}(\boldsymbol{n}) = \tilde{\boldsymbol{c}}^T(\boldsymbol{n})\boldsymbol{x}(\boldsymbol{n}) = \tilde{\boldsymbol{c}}^T(\boldsymbol{n})\boldsymbol{M}^{-1}\boldsymbol{M}\boldsymbol{x}(\boldsymbol{n}) = \boldsymbol{\phi}^T(\boldsymbol{n})\boldsymbol{y}(\boldsymbol{n})$$
$$\boldsymbol{v}(\boldsymbol{n}) = \boldsymbol{c}(\boldsymbol{n})\boldsymbol{u}(\boldsymbol{n}),$$

where $\tilde{\boldsymbol{c}} = \boldsymbol{c}$ typically and $\boldsymbol{\phi} \equiv \boldsymbol{M}^{-T}\tilde{\boldsymbol{c}}$. Most luminance-chrominance decompositions are designed such that $y_2 = y_3 = 0$ when $x_1 = x_2 = x_3$. Consequently, it can readily be shown that $\phi_2(\boldsymbol{n})$ and $\phi_3(\boldsymbol{n})$ are pure sinusoids, where the corresponding frequencies are $(\frac{2\pi}{3}, 0)$ and $(\frac{2\pi}{3}, \frac{2\pi}{3})$ for vertical and diagonal stripe sampling, respectively. Thus, the Fourier transform of the stimuli is a sum of the chrominance signals modulated by $(\frac{2\pi}{3}, 0)$ or $(\frac{2\pi}{3}, \frac{2\pi}{3})$ and the luminance signal. Figures 1(d-e) show example spectra, revealing severe aliasing between the luminance and the chrominance components near the modulation frequencies.

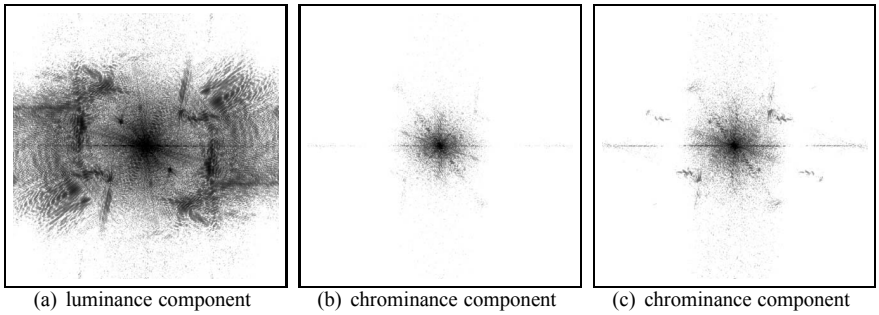

(a) luminance component (b) chrominance component (c) chrominance component

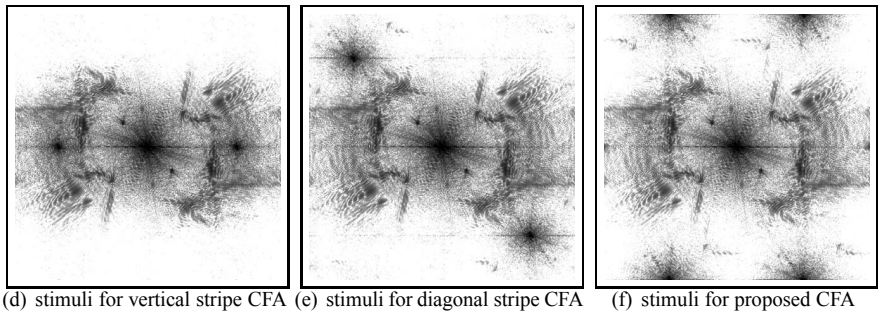

(d) stimuli for vertical stripe CFA (e) stimuli for diagonal stripe CFA (f) stimuli for proposed CFA

Fig. 1. 2D Fourier transform of "Barbara." The log-magnitude of coefficients displayed as pixel intensity. DC is found in the center.

3. DESIGN AND ANALYSIS OF NEW CFA PATTERNS

3.1. A New Alternative to Existing CFA Patterns

Let $h_i(\boldsymbol{n})$ be the CSF for $y_i(\boldsymbol{n})$ and '$*$' denotes convolution. Then the low-level human visual response to a color image $\boldsymbol{x}(\boldsymbol{n})$ is $\boldsymbol{\mathcal{W}}(\boldsymbol{x}) = (\mathcal{W}_1(\boldsymbol{x}), \mathcal{W}_2(\boldsymbol{x}), \mathcal{W}_3(\boldsymbol{x}))$ where $\mathcal{W}_i(\boldsymbol{x})(\boldsymbol{n}) = h_i(\boldsymbol{n}) * y_i(\boldsymbol{n})$. Recall that multiplication in the spatial domain implicates a convolution in the Fourier domain, and assume that the passband of h_i is wide enough such that $h_i(\boldsymbol{n}) * y_i(\boldsymbol{n}) = y_i(\boldsymbol{n})$. Our objective is to choose $\{\boldsymbol{c}, \tilde{\boldsymbol{c}}\}$ such that $\boldsymbol{\mathcal{W}}(\boldsymbol{x}) = \boldsymbol{\mathcal{W}}(\boldsymbol{v})$. To do so, let us examine the properties of $\boldsymbol{\mathcal{W}}(\boldsymbol{v})$:

$$\begin{aligned}\mathcal{W}_i(\boldsymbol{v})(\boldsymbol{n}) =& h_i(\boldsymbol{n}) * z_i(\boldsymbol{n})\\ \boldsymbol{z}(\boldsymbol{n}) \equiv& \boldsymbol{M}\boldsymbol{v}(\boldsymbol{n}) = \boldsymbol{M}\boldsymbol{c}(\boldsymbol{n})\boldsymbol{u}(\boldsymbol{n}) = \boldsymbol{\psi}(\boldsymbol{n})\boldsymbol{\phi}^T(\boldsymbol{n})\boldsymbol{y}(\boldsymbol{n}),\end{aligned}$$

where $\boldsymbol{\psi} = \boldsymbol{M}\boldsymbol{c}$. Then our condition can be rewritten as:

$$y_i(\boldsymbol{n}) \approx h_i(\boldsymbol{n}) * (\psi_i(\boldsymbol{n})\boldsymbol{\phi}^T(\boldsymbol{n})\boldsymbol{y}(\boldsymbol{n})). \tag{1}$$

Let $\phi_i(\boldsymbol{n}) = k_i\psi_i(\boldsymbol{n})$ for some constant k_i. Then (1) can be viewed as a classical amplitude modulation problem, where multiple signals of interest are transmitted over the same media by modulating first via the multiplication in the time domain. Thus the carrier frequencies $\psi_i = \phi_i$ must be chosen such that:

- $h_i(\boldsymbol{n}) * (\psi_i(\boldsymbol{n})\phi_j(\boldsymbol{n})) = 1$ when $i = j$;
- $h_i(\boldsymbol{n}) * (\psi_i(\boldsymbol{n})\phi_j(\boldsymbol{n})) = 0$ when $i \neq j$;
- $\boldsymbol{u} = \phi_1 y_1 + \phi_2 y_2 + \phi_3 y_3$ is alias free;
- $\boldsymbol{u} \geq 0$.

More specifically, when $i \neq j$ we would like the frequency contents of $\psi_i(\boldsymbol{n})\phi_j(\boldsymbol{n})$ to be sufficiently high such that $\psi_i(\boldsymbol{n})\phi_j(\boldsymbol{n})y_j(\boldsymbol{n})$ is outside the passband for $h_i(\boldsymbol{n})$. Since the bandwidth of $y_1(\boldsymbol{n})$ is the largest, we set $\phi_1(\boldsymbol{n}) = k_1\psi_1(\boldsymbol{n}) = 1, \forall \boldsymbol{n}$. Our strategy is to modulate y_2 and y_3 via the multiplication with ϕ_2 and ϕ_3 such that the 2D Fourier transform of the frequency-modulated chrominance signals occupy the regions in the frequency domain not used by y_1.

Below, we design $\boldsymbol{\phi}$ and $\boldsymbol{\psi}$ in the frequency domain, take their inverse Fourier transforms to find the equivalent representation in the spatial domain, and compute $\tilde{\boldsymbol{c}} = \boldsymbol{M}^T\boldsymbol{\phi}$ and $\boldsymbol{c} = \boldsymbol{M}^{-1}\boldsymbol{\psi}$. Let us begin by assuming that $\{\phi_2, \phi_3\}$ have two-dimensional Fourier transform of the following from:

$$\begin{aligned}\mathcal{F}(\phi_2)(\boldsymbol{\omega}) &= \sum_i s_i\delta(\boldsymbol{\omega} + \boldsymbol{\tau}_i) + \bar{s}_i\delta(\boldsymbol{\omega} - \boldsymbol{\tau}_i)\\ \mathcal{F}(\phi_3)(\boldsymbol{\omega}) &= \sum_i t_i\delta(\boldsymbol{\omega} + \boldsymbol{\tau}_i) + \bar{t}_i\delta(\boldsymbol{\omega} - \boldsymbol{\tau}_i)\end{aligned} \tag{2}$$

where $\boldsymbol{\tau}_i \in \mathbb{R}^2$, $\delta(\cdot)$ is the Dirac delta function, and $\bar{s}_i$ denotes complex conjugate of s_i. Note that the symmetry properties in (2) guarantees that the inverse Fourier transform is real. Then, the overall Fourier tranform of the stimuli is a sum of luminance and frequency-modulated chrominances:

$$\begin{aligned}\mathcal{F}(\boldsymbol{u}) &= \mathcal{F}(\boldsymbol{\phi}^T\boldsymbol{y})\\ &= \mathcal{F}(y_1)(\boldsymbol{\omega}) + \sum_i (s_i\mathcal{F}(y_2) + t_i\mathcal{F}(y_3))(\boldsymbol{\omega} + \boldsymbol{\tau}_i)\\ &\quad + \sum_i (\bar{s}_i\mathcal{F}(y_2) + \bar{t}_i\mathcal{F}(y_3))(\boldsymbol{\omega} - \boldsymbol{\tau}_i).\end{aligned}$$

Note that the design parameters of the color filter consist of carrier frequencies $\{\boldsymbol{\tau}_i\}$ and their weights $\{s_i, t_i\}$. Ideally, the optimal CFA pattern achieves partitioning of $y_1(\boldsymbol{n}), y_2(\boldsymbol{n}), y_3(\boldsymbol{n})$ in the frequency domain representation of the stimuli. By choosing a carrier $\boldsymbol{\tau}_i$ sufficiently far from the baseband (i.e., high-frequency), the chances of $\phi_2 y_2$ and $\phi_3 y_3$ overlapping with $\phi_1 y_1$ in the frequency domain is minimized while $\psi_1\phi_2$, $\psi_1\phi_3$, $\psi_2\phi_1$, and $\psi_3\phi_1$ fall outside of the passband for h_1, h_1, h_2, and h_3, respectively. As a result, the *effective* spatial resolution of image display is increased because

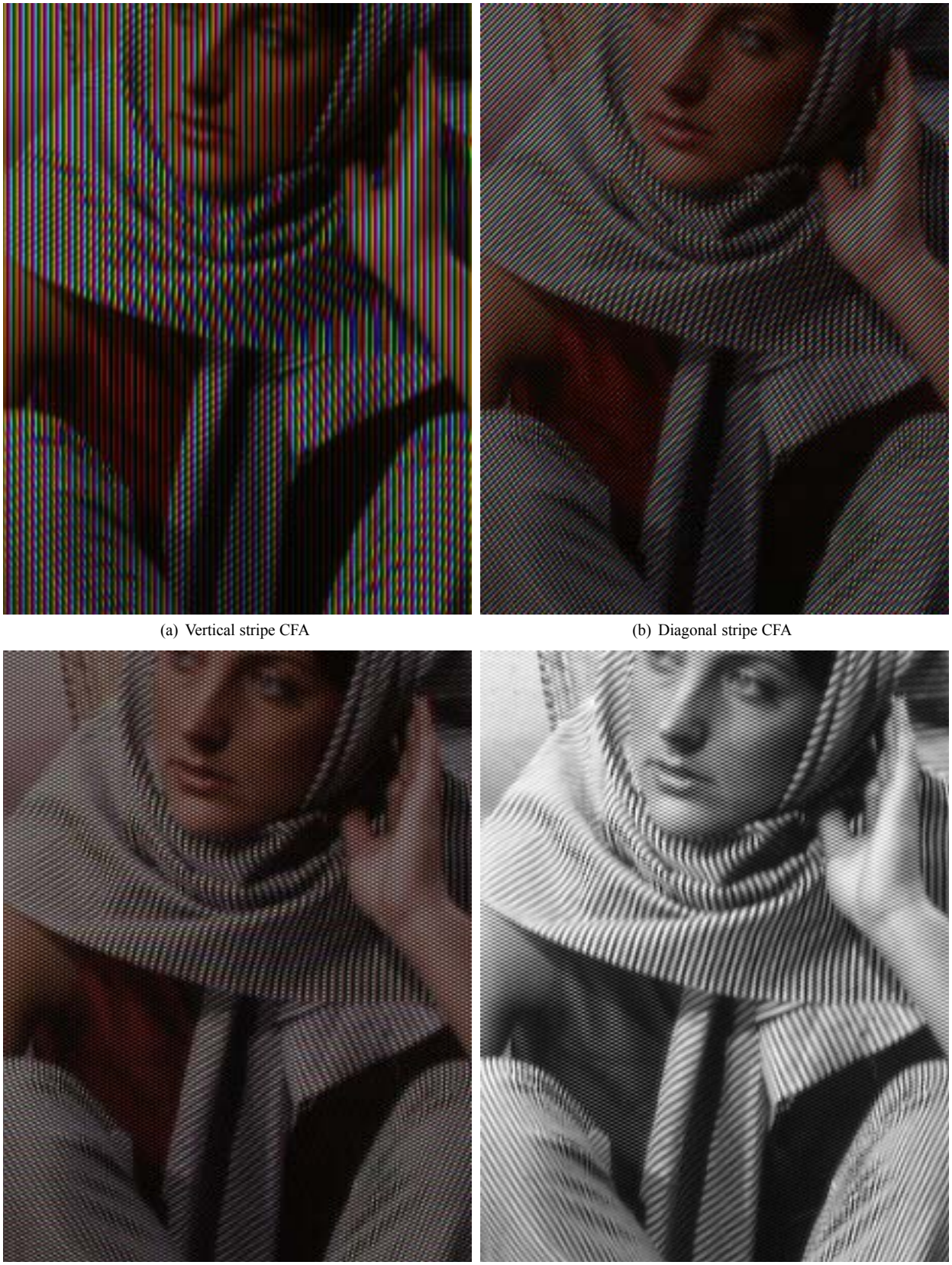

(a) Vertical stripe CFA

(b) Diagonal stripe CFA

(c) Proposed CFA

(d) Stimuli for proposed

Fig. 3. Example output using "Barbara." The figure *must* be viewed on screen with 96dpi scaled at 100%.

the size of the areas in $\mathcal{F}(y_1)$ that do not overlap with the modulated chrominance signals are far larger than that of the existing CFA patterns. Furthermore, a CFA pattern with the carrier frequencies fixed away from DC is consequently less sensitive to the directionality of the image features.

The requirement that $\boldsymbol{u}$ be non-negative can be met by setting $\{s_i, t_i\}$ relatively small compared to the DC value (compensated for by k_2 and k_3). Furthermore, the choice of carrier frequencies may be restricted to rational multiples of π so that the inverse Fourier transform of (2) is periodic. For example, $\boldsymbol{\tau}_i$ lying on multiples of $\frac{\pi}{2}$ induces a 4×4 CFA pattern. One unique aspect of the proposed CFA scheme is that the resulting pattern does not consist of pure red, green, and blue samples, but rather of a mixture at every subpixel position.

3.2. Implementation and Examples

A design of CFA pattern satisfying the proposed design criteria set forth in section 3.1 is not unique. In order to evaluate the output image independent of the pixel geometry, we assume square pixels arranged in a rectangular lattice. Generalization to subpixel rendering and other pixel geometries is straightforward. Likewise, anti-aliasing measures are purposely not taken, in order to illustrate the fundamental throughput of the stimuli signal. Consider a CFA pattern induced with the following parameters:

$$\boldsymbol{M} = \begin{bmatrix} 0.5774 & 0.5774 & 0.5774 \\ -0.5774 & 0.7887 & -0.2113 \\ -0.5774 & -0.2113 & 0.7887 \end{bmatrix}$$

$$\mathcal{F}(\phi_2)(\boldsymbol{\omega}) = \frac{3+3i}{8}\delta(\boldsymbol{\omega} + (\frac{\pi}{2}, \pi)^T) + \frac{3-3i}{8}\delta(\boldsymbol{\omega} - (\frac{\pi}{2}, \pi)^T)$$

$$\mathcal{F}(\phi_3)(\boldsymbol{\omega}) = \frac{3-3i}{8}\delta(\boldsymbol{\omega} + (\frac{\pi}{2}, \pi)^T) + \frac{3+3i}{8}\delta(\boldsymbol{\omega} - (\frac{\pi}{2}, \pi)^T).$$

The proposed pattern implies a periodic structure of size 2×4. and though as it appears on Figure 2 that it consists of the usual red, green, and blue in addition to light blue, every color in this figure is actually a mixture of all primaries (it is easy to verify that arranging red, green, blue plus a fourth color in similar 2×4 lattice pattern would result in a sub-optimal performance).

Figure 3 shows an example stimuli and display of a widely available color image, "Barbara," using the above pattern. As apparent from the figure, the vertical stripe CFA is subject to severe aliasing in high-frequency regions such as the scarf and the pants of "Barbara" image. Although the diagonal stripe CFA is a clear improvement over the vertical, it is unable to supress the aliasing completely in the textured regions. The proposed CFA, however, is able to resolve the high-frequency content of the image. In particular, the textures on the scarf and the pants, which are oriented in many directions, are recognizable without major artifacts. The improvements in Figure 3 can be explained via the Fourier transform of the stimuli $\boldsymbol{u}$ in Figure 1(f). As the distance between DC and the frequency-modulated chrominance signals in the two-dimensional Fourier domain are far greater, we see that aliasing is much less likely to have occured.

Additionally, the stimuli $\boldsymbol{u}(\boldsymbol{n})$ (figure 3(d)) can be regarded as a grayscale representation of the color image $\boldsymbol{x}(\boldsymbol{n})$ with additional information about its chromaticity content embedded inside low-visibility, high-frequency textures. Such mapping gives rise to a reversible coding of color images in black-and-white prints, a technique proven useful in scanning and printing applications [13]. Owing to length constraints, a detail discussion of this point is omitted.

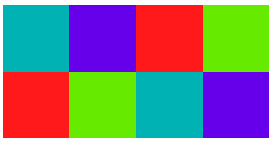

Fig. 2. Induced CFA pattern.

4. CONCLUSION

In this paper, we proposed to evaluate the display device CFA in terms of throughput of stimuli as limited by aliasing. We showed that the the spectral replicas of the chrominance signals induced by existing CFA patterns are centered around frequencies that are not sufficiently far from the DC, consequently overlapping with the luminance signal spectrum and reducing the throughput of the stimuli. We reinterpret the interactions between the stimuli, display CFA, and CSF in terms of amplitude modulation, and offer an alternative CFA coding scheme that modulates the chrominance signals to a higher frequency relative to common schemes.

5. REFERENCES

[1] R. L. De Valois and K. De Valois, *Spatial Vision*, Oxford University Press, 1990.

[2] O. H. Schade, "Optical and photoelectric analog of the eye," *J. Opt. Soc. Am.*, , no. 46, pp. 721–739, Sep 1956.

[3] B. Wandell and L. D. Silverstein, "Digital color reproduction," in *The Science of Color*, S. Shevell, Ed., pp. 281–316. Optical Society of America, 2003.

[4] J. F. Blinn, "What is a pixel?," *IEEE Computer Graphics and Applications*, vol. 25, no. 5, pp. 82–87, Sep-Oct 2005.

[5] D. S. Messing, L. Kerofsky, and S. Daly, "Subpixel rendering on nonstriped colour matrix displays," in *Proc. IEEE Internat. Conf. Image Processing*, 2003, vol. 2, pp. 949–952.

[6] J. Pollack, "Displays of a different stripe," *IEEE Spectrum*, vol. 43, no. 8, pp. 40–44, 2006.

[7] G. Sharma and H. J. Trussell, "Digital color imaging," *IEEE Trans. Image Processing*, vol. 6, no. 7, pp. 901–932, 1997.

[8] D. Taubman, "Generalized wiener reconstruction of images from colour sensor data using a scale invariant prior," in *Proc. IEEE Internat. Conf. Image Processing*, 2000, vol. 3, pp. 801–804.

[9] K. Hirakawa and T. W. Parks, "Adaptive homogeneity-directed demosaicing algorithm," *IEEE Trans. Image Processing*, vol. 14, no. 3, pp. 360–369, March 2005.

[10] K. Hirakawa and T. W. Parks, "Joint demosaicing and denoising," *IEEE Trans. Image Processing*, vol. 15, no. 8, pp. 2146–2157, August 2006.

[11] B. K. Gunturk, Y. Altunbasak, and R. M. Mersereau, "Color plane interpolation using alternating projections," *IEEE Trans. Image Processing*, vol. 11, no. 9, pp. 997–1013, September 2002.

[12] R. Lukac and K. N. Plataniotis, "Color filter arrays: Design and performance analysis," *IEEE Trans. Consumer Electronics*, vol. 51, no. 4, pp. 1260–1267, November 2005.

[13] K. M. Braun R. L. de Queiroz, "Color to gray and back: Color embedding into textured gray images," *IEEE Trans. Image Processing*, vol. 15, no. 6, pp. 1464–1470, June 2006.